

Comparison of Approximate Momentum Equations in Dynamic Models of Vapor Compression Systems

Qiao, H.; Laughman, C.R.

TR2018-131 August 31, 2018

Abstract

Model reduction techniques are often applied to improve the computational speed when finite volume models are used to describe the dynamics of heat exchangers (HXs) in vapor compression systems. One particular area of focus has been the simplification of the momentum equation, since it usually does not affect the thermal system behavior over the time scales of interest. This paper compares the effect of five reduced order variants of the momentum equation on the dynamics of complete vapor compression cycles. This comparison is achieved via the implementation of a dynamic model of an air-source heat pump, which enables the direct comparison of these different approximations on the system dynamics, prediction accuracy, and simulation speed on otherwise identical models. Simulations indicate that neglecting the phenomena on small time scales can greatly improve numerical efficiency with a minimal loss in prediction accuracy. The variants with frictional pressure drop only and with linear pressure distribution are also found to outperform other variants in both prediction accuracy and simulation speed.

International Heat Transfer Conference

This work may not be copied or reproduced in whole or in part for any commercial purpose. Permission to copy in whole or in part without payment of fee is granted for nonprofit educational and research purposes provided that all such whole or partial copies include the following: a notice that such copying is by permission of Mitsubishi Electric Research Laboratories, Inc.; an acknowledgment of the authors and individual contributions to the work; and all applicable portions of the copyright notice. Copying, reproduction, or republishing for any other purpose shall require a license with payment of fee to Mitsubishi Electric Research Laboratories, Inc. All rights reserved.

COMPARISON OF APPROXIMATE MOMENTUM EQUATIONS IN DYNAMIC MODELS OF VAPOR COMPRESSION SYSTEMS

Hongtao Qiao* & Christopher R. Laughman

¹Mitsubishi Electric Research Laboratories, Cambridge, MA 02139, USA

ABSTRACT

Model reduction techniques are often applied to improve the computational speed when finite volume models are used to describe the dynamics of heat exchangers (HXs) in vapor compression systems. One particular area of focus has been the simplification of the momentum equation, since it usually does not affect the thermal system behavior over the time scales of interest. This paper compares the effect of five reduced order variants of the momentum equation on the dynamics of complete vapor compression cycles. This comparison is achieved via the implementation of a dynamic model of an air-source heat pump, which enables the direct comparison of these different approximations on the system dynamics, prediction accuracy, and simulation speed on otherwise identical models. Simulations indicate that neglecting the phenomena on small time scales can greatly improve numerical efficiency with a minimal loss in prediction accuracy. The variants with frictional pressure drop only and with linear pressure distribution are also found to outperform other variants in both prediction accuracy and simulation speed.

KEY WORDS: Heat transfer, Dynamic modeling, Momentum balance, Vapor compression system, Modelica

1. INTRODUCTION

Heat exchangers in vapor compression systems usually require particular modeling attention, because they are the main components that exchange mass, energy and momentum in the system. It is therefore essential to obtain accurate mathematical and physical representations for transient heat transfer and fluid flow phenomena in the heat exchangers. Distributed-parameter heat exchanger models are particularly useful for describing spatially dependent phenomena and the detailed component performance, such as the effect of local heat transfer coefficients and pressure drops or the branching and joining of refrigerant pipes as a result of particular circuiting configurations. In such models, the original governing equations for one-dimensional fluid flow in a form of partial differential equations are spatially discretized and can be solved by various methods like finite difference, finite volume or finite element methods. While the finite volume method is often chosen because it can accurately maintain conserved quantities, this high accuracy is achieved at a cost of longer simulation time. Model reduction techniques are thus often needed to improve the computational speed of the models.

One particular area of focus has been the simplification of the momentum equation, since it usually does not affect the thermal system behavior over the time scales of interest; in this work, we study five simplified variants of the momentum equation used in the dynamic modeling of HXs that have been reported in the literature. The standard transient momentum equation includes the inertia term which contains the time-derivative of the mass flow rate and is important for describing the propagation of pressure fluctuations and other effects of very small time scales. Typically, this term is of minor importance for heat transfer analysis, and often involves

*Corresponding Hongtao Qiao: qiao@merl.com

a much shorter time constant than the thermal transport behavior. Including this inertia term in the models often leads to a stiff system of differential equations and significantly increases the computational cost. Meanwhile, the physical phenomena that the inertia term describes are of no interest to system modelers unless sound or shock waves inside a tube need to be taken into account [1]. Consequently, in the first simplified variant of the momentum equation, the inertia term is often neglected. In the second variant, the acceleration term and the gravity effect are also omitted, as these terms are usually much smaller than the friction term [2]. In comparison, the third variant assumes that the time derivatives of the pressures are spatially invariant in the heat exchanger due to the fact that the dynamic pressure waves propagate at the speed of sound in the direction of fluid flow [3]. The fourth variant applies a global momentum balance by assuming a linear pressure distribution across all the volumes between the inlet and the outlet of the heat exchanger [4]. In addition to these four simplified variants of the momentum equation, the spatial variation of the pressure is often neglected in many studies to avoid the resulting complexity due to the inclusion of the momentum equation in the models (the 5th variant) [5]. In this variant, pressure will be uniform throughout the heat exchanger and the mass flow rate will be computed through the coupling between the equations of continuity and energy.

Zhang and Zhang [6] compared three different forms of the momentum equation in the dynamic simulation of a residential refrigeration system: standard/transient, steady-state (1st variant) and zero pressure drop (5th variant). It was concluded that the steady-state form yielded the same prediction as the standard form while maintaining a faster computation speed. The authors also suggest that pressure drop can reasonably be neglected in model-based control design, since it results in a simpler model representation without a significant loss of accuracy. However, zero pressure drop assumption cannot be justified in some cases, such as electronics cooling, where micro channels are commonly used and significant pressure drop can be observed in micro-scale heat exchangers, and large-scale heat exchangers in solar thermal plants (tube length can be as long as hundreds of meters), where pressure drop must be considered. In addition, the momentum balance must be taken into account to determine the mass flow interactions between the evaporators when it comes to the modeling of multi-evaporator systems. Because the evaluation of the steady-state momentum equation is still quite computationally expensive, the other three simpler variants (2nd, 3rd and 4th variants) may be more favorable alternatives in the dynamic simulation of vapor compression systems to attain a trade-off between numerical efficiency and preservation of the major physical characteristics.

Unfortunately, while all these different variants of the momentum equation have been used in previous literature, their computational speed and accuracy have not been directly compared. In this paper, we will compare the effect of these model-order reduction strategies on the dynamics of complete vapor compression cycles, thereby directly establishing the tradeoffs between computational speed and accuracy. This comparison is achieved via the implementation of a dynamic model of an air-source heat pump in the equation-oriented language Modelica, which enables the direct comparison of these different approximations of the momentum equation on the system dynamics, prediction accuracy, and simulation speed on otherwise identical models.

2. MODEL DEVELOPMENT

The heat exchangers are described by a finite-volume model of the heat and fluid flow. Each heat exchanger segment is divided into three sections: the refrigerant stream, the finned walls, and the air stream. The refrigerant stream is described by a one-dimensional flow with fluid properties varying only in the direction of flow; consequently, these properties are uniform or averaged at every cross section along the axis of the channel. Additional assumptions used to simplify the dynamic models include: (1) the fluid is Newtonian, (2) axial heat conduction in the direction of refrigerant flow is ignored, (3) viscous dissipation is neglected, (4) liquid and vapor are in thermodynamic equilibrium, (5) the potential and kinetic energy of the refrigerant is neglected. The conservation equations of continuity, energy and momentum can thus be formulated as follows [7]:

$$A_c \frac{\partial \bar{\rho}}{\partial t} + \frac{\partial \dot{M}}{\partial z} = 0 \quad (1)$$

$$\frac{\partial(\bar{\rho}\bar{h}_\rho A_c)}{\partial t} + \frac{\partial(\dot{M}\bar{h})}{\partial z} = Pq'' + \frac{\partial(pA_c)}{\partial t} \quad (2)$$

$$\frac{\partial\dot{M}}{\partial t} + \frac{\partial}{\partial z} \left(\frac{\dot{M}|\dot{M}|}{\bar{\rho}_M A_c} \right) = -A_c \frac{\partial p}{\partial z} - P\bar{\tau}_w - \bar{\rho}gA_c \sin\theta \quad (3)$$

where $\bar{\rho}_M$ is the momentum density. \bar{h}_ρ and \bar{h} are the density-weighted and flow-weighted specific enthalpies, respectively. The wall shear stress $\bar{\tau} = \frac{1}{2}f\bar{\rho}u|u|$ and f is the Fanning friction factor, while P is the circumference of the flow channel. Please note a symbol with a bar represents an average value in this paper.

In order to apply the finite volume method to solve the governing equations, the domain of the refrigerant flow needs to be spatially discretized into n control volumes. The staggered grid scheme is used to decouple the equations of continuity and energy with the equation of momentum. There are two types of cells: volume cells (blocks enclosed in black solid lines), and flow cells (blocks enclosed in red dash lines) centered at the interfaces of the volume cells, as shown in Fig. 1. The mass and energy balances are calculated within the volume cell while the momentum balance is calculated between the volume cells, i.e., within the flow cell. Integrating the equations of continuity and energy over the i^{th} volume cell yields

$$A_c \Delta z \left(\frac{\partial \bar{\rho}_i}{\partial p_i} \frac{dp_i}{dt} + \frac{\partial \bar{\rho}_i}{\partial \bar{h}_{\rho,i}} \frac{d\bar{h}_{\rho,i}}{dt} \right) = \dot{M}_{i-1/2} - \dot{M}_{i+1/2}, \quad (4)$$

$$A_c \Delta z \left(\bar{\rho}_i \frac{d\bar{h}_{\rho,i}}{dt} - \frac{dp_i}{dt} \right) = \dot{M}_{i-1/2} (h_{i-1/2} - \bar{h}_{\rho,i}) - \dot{M}_{i+1/2} (h_{i+1/2} - \bar{h}_{\rho,i}) + P \Delta z q_i'' \quad (5)$$

It is also necessary to relate the quantities between the volume and flow cells, e.g.,

$$\varphi_{i+1/2} \approx \delta_i \varphi_i + (1 - \delta_i) \varphi_{i+1}. \quad (6)$$

The upwind difference scheme is recommended to approximate thermodynamic quantities onto the staggered cells for convection-dominated flows, because the central difference scheme may lead to non-physical solutions [8].

$$\delta_i = \begin{cases} 1 & \dot{M}_{i+1/2} \geq 0 \\ 0 & \dot{M}_{i+1/2} < 0 \end{cases} \quad (7)$$

The standard/transient form of the momentum equation for the i^{th} flow cell is thus

$$\Delta z \frac{d\dot{M}_{i+1/2}}{dt} = \dot{I}_i - \dot{I}_{i+1} - A_c(p_{i+1} - p_i) - P \Delta z \bar{\tau}_{w,i+1/2} - \bar{\rho}_{i+1/2} g A_c \Delta z \sin\theta_i. \quad (8)$$

The momentum at the interfaces of flow cells is often calculated using a second-order center difference in order to avoid the discontinuity caused by the reverse flow, i.e., $\delta = 1/2$ in this case

$$\dot{I}_i - \dot{I}_{i+1} = \frac{(\dot{I}_{i-1/2} + \dot{I}_{i+1/2})}{2} - \frac{(\dot{I}_{i+1/2} + \dot{I}_{i+3/2})}{2} = \frac{1}{2}(\Delta \dot{I}_i + \Delta \dot{I}_{i+1}), \quad (9)$$

where $\Delta \dot{I}$ is the momentum flow difference across the flow cell, e.g., $\Delta \dot{I}_i = \dot{I}_{i-1/2} - \dot{I}_{i+1/2}$, \dot{I} is the momentum flow, e.g., $\dot{I}_{i+1/2} = \dot{M}_{i+1/2} |\dot{M}_{i+1/2}| / (\bar{\rho}_{M,i+1/2} A_c)$, and half of the last flow cell is outside the refrigerant pipe. The momentum difference across the last flow cell is therefore approximated as that across the last volume cell, i.e., $\dot{I}_n - \dot{I}_{n+1} \approx \dot{I}_{n-1/2} - \dot{I}_{n+1/2}$. Pressure p , the density-weighted enthalpy \bar{h}_ρ and mass flow rate \dot{M} are the dynamic states. The boundary conditions are the mass flow rate and specific enthalpy at the inlet, and the pressure at the outlet, i.e., $\dot{M}_{1/2}$, $h_{1/2}$ and p_{n+1} . In total, there will be $3n$ ordinary differential equations for a pipe with n control volumes. As can be seen from the derivations described above, employing the standard momentum equation in the models adds significant computational complexity. As a result, a variety of numerical approaches have been introduced in the literature to simplify the analyses and accelerate

the simulation speed while maintaining physical integrity. The detailed description of these simplified variants of the momentum equation is given below.

Variant 1: Steady-state form The derivative in Eq.(8) is the inertia term, and can be neglected due to its minor importance for heat transfer analysis. Consequently, the steady-state form of the momentum equation becomes [1]

$$0 = \dot{I}_i - \dot{I}_{i+1} - A_c(p_{i+1} - p_i) - P\Delta z \bar{\tau}_{w,i+1/2} - \bar{\rho}_{i+1/2} g A_c \Delta z \sin\theta_i. \quad (10)$$

The resultant momentum equation is substantially simplified by eliminating the inertia term. Compared against the standard form, the number of dynamic states with the steady-state form reduces to $2n$ (pressures and specific enthalpies) since the mass flow rates become the algebraic variables.

Variant 2: Frictional pressure drop only The steady-state momentum equation can be further reduced by neglecting the acceleration pressure drop and gravity effect [2], since both of them are typically smaller than the frictional pressure drop, yielding

$$p_{i+1} = p_i - \frac{P}{A_c} \Delta z \bar{\tau}_{w,i+1/2}. \quad (11)$$

In this variant, we assume that the number of states are still $2n$ and the mass flow rates are the algebraic variables.

Variant 3: dp/dt approach In this variant, the time derivatives of pressures are spatially invariant along the direction of flow given that the acoustic waves propagate with a speed of sound in the direction of fluid flow. As a result, the number of dynamic pressure states is reduced to a single numerical state per pressure level, yielding a very efficient system of equations for each control volume, since dp/dt is given as an input. It is important to note that the time derivative of pressure is not treated as constant over time, but rather in space along the direction of flow. The pressure distribution in the heat exchanger still depends on the selected pressure drop models and thus on the mass flow rates [3]. Since $\frac{dp_1}{dz} = \frac{dp_{n+1}}{dz} = \frac{dp_{ref}}{dz}$, the equations of continuity and energy become

$$A_c \Delta z \left(\frac{\partial \bar{\rho}_i}{\partial p_i} \frac{dp_{ref}}{dt} + \frac{\partial \bar{\rho}_i}{\partial \bar{h}_{\rho,i}} \frac{d\bar{h}_{\rho,i}}{dt} \right) = \dot{M}_{i-1/2} - \dot{M}_{i+1/2} \quad (12)$$

$$A_c \Delta z \left(\bar{\rho}_i \frac{d\bar{h}_{\rho,i}}{dt} - \frac{dp_{ref}}{dt} \right) = \dot{M}_{i-1/2} (h_{i-1/2} - \bar{h}_{\rho,i}) - \dot{M}_{i+1/2} (h_{i+1/2} - \bar{h}_{\rho,i}) + P \Delta z q_i'' \quad (13)$$

In this approach, only specific enthalpies are the differential variables, and therefore the total number of dynamic states is reduced by $n-1$. Meanwhile, this approach can possibly avoid stiff models by eliminating a large number of fast pressure states. The algebraic dependency of pressure drop on the mass flow can be removed by introducing pseudo continuous time states that follow the steady-state pressure drops with delay [1].

$$\frac{d\Delta p_{i,state}}{dt} = -\frac{1}{K_{state}} (\Delta p_{i,state} - \Delta p_{i,cal}) \quad (14)$$

where $\Delta p_{i,state} = p_i - p_{i+1}$, $\Delta p_{i,cal}$ is the steady-state frictional pressure drop calculated using correlations, and K_{state} is the time constant that can be tuned. With the introduction of pseudo pressure drop states, the number of dynamic states increases to $2n+1$, but the numerical efficiency of the approach is greatly improved.

Variant 4: Linear pressure distribution Another means of decreasing the number of dynamic states is to assume that the pressure is linearly distributed along the heat exchanger [4], i.e., $p_i = p_1 + (i-1) \frac{p_{n+1} - p_1}{n}$. Therefore, one can easily obtain the following

$$\frac{dp_i}{dt} = \left(1 - \frac{i-1}{n}\right) \frac{dp_1}{dt} + \frac{i-1}{n} \frac{dp_{n+1}}{dt} \quad (15)$$

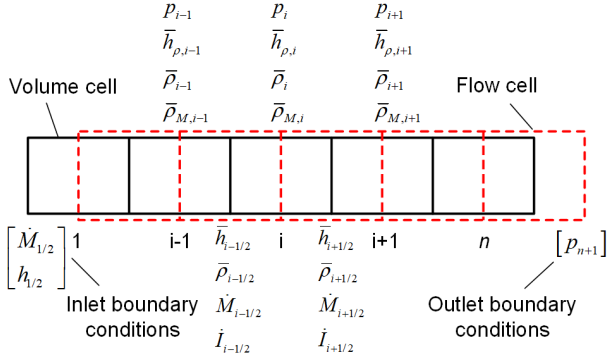


Fig. 1 Finite volume discretization of refrigerant pipe.

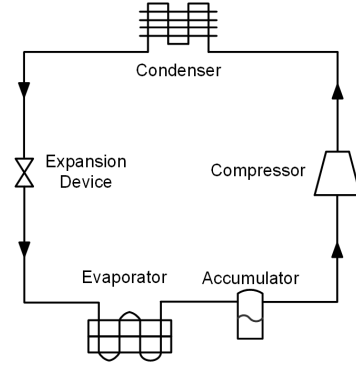


Fig. 2 Schematic diagram of air-source heat pump.

Aggregating all local momentum balances for flow cells 1 to n results in

$$n\Delta z \frac{d\bar{M}}{dt} = \dot{I}_1 - \dot{I}_{n+1} - A_c(p_{n+1} - p_1) - P\Delta z \sum_{i=1}^n \bar{\tau}_{w,i+1/2} - gA_c\Delta z \sum_{i=1}^n \bar{\rho}_{i+1/2} \sin\theta_i \quad (16)$$

where \bar{M} is the average mass flow rate $\frac{1}{n} \sum_{i=1}^n \dot{M}_{i+1/2}$. This variant can be further simplified by summing up the momentum equation with only frictional pressure drop instead for all the flow cells. Similarly, a pseudo total pressure drop state can be introduced to remove the dependency of pressure drop on mass flow rate.

$$\frac{d}{dt} \Delta p_{tot,state} = -\frac{1}{K_{state}} (\Delta p_{tot,state} - \sum_{i=1}^n \Delta p_{i,cal}) \quad (17)$$

where $\Delta p_{tot,state} = p_1 - p_{n+1}$. This variant only has $n+3$ dynamic states.

Variant 5: Zero pressure drop In many cases, pressure drop across the heat exchanger is very small and can be neglected [5]. With this assumption, the momentum equation is not required in the analysis and the number of dynamic states is $n+1$. The mass flow rates will be computed through the coupling between the equations of mass and energy. The boundary conditions of this approach are the inlet enthalpy, inlet and outlet mass flow rates, i.e., $h_{1/2}$, $\dot{M}_{1/2}$ and $\dot{M}_{n+1/2}$.

3. RESULTS AND DISCUSSIONS

An air source heat pump cycle was constructed to enable the direct comparison of these different approximations of the momentum equation on the system dynamics, prediction accuracy and simulation speed. The heat pump system used R134A as the working fluid, and consisted of a condenser, an evaporator, a linear electronic expansion valve (LEV), and an accumulator and scroll compressor, as shown in Fig. 2. The compressor was a low-side scroll compressor with displacement of 66.7 cm^3 and nominal rotational speed of 3500 rpm, and both heat exchangers were louvered fin-and-tube heat exchangers. The modeling techniques of the air side and tube walls are given in [9], and the details of the supporting component models including compressor, accumulator and LEV models can be found in [10]. These models were augmented by a set of empirical closure relations describing the single- and two-phase heat transfer coefficients and frictional pressure drops for the fluid on both the refrigerant side and the air-side [9]. The Levy void fraction model [11] was used to compute the two-phase refrigerant mass inventory. A tube-by-tube approach was employed for the heat exchanger analysis, i.e., the performance of each tube was analyzed separately and each tube was associated with different refrigerant and air parameters. These models were implemented in the Modelica language using the Dymola 2017 simulation environment, and were run on a laptop with an Intel i7 processor and 32 Gb of RAM; the Radau IId solver was used to integrate the set of differential algebraic equations with a tolerance of $1e-5$.

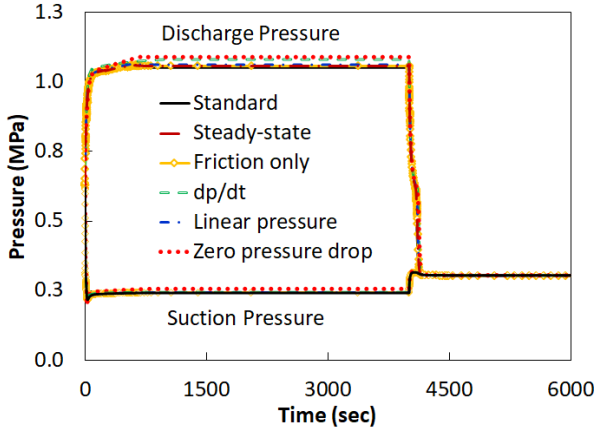


Fig. 3 Comparison of pressure transients between approximation methods.

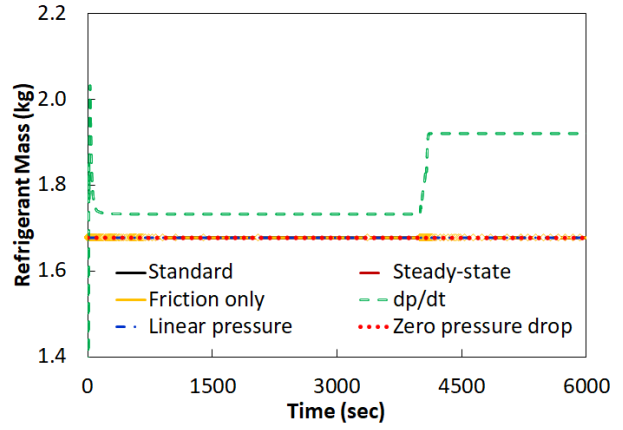


Fig. 4 Comparison of refrigerant mass between approximation methods.

As the first step towards the comparison of these different variants of the momentum equation, a complete start-stop cycle of the heat pump system was simulated. The dynamic system model was initialized with an equilibrium system pressure of 0.63MPa to mimic the scenario that the heat pump had been shut down for some time, with a majority of refrigerant residing in the evaporator and accumulator. The total simulation time lasted 6000 sec, with 4000 sec on-period and 2000 sec off-period, respectively. The comparison of the pressure transients using different variants of the momentum equation was given in Fig. 3. Within the first 2 minutes, the discharge pressure increased rapidly, then gradually slowed down the ascending trend and leveled off. The surge in the discharge pressure was mainly attributed to the imbalance between the mass flow entering and leaving the condenser. The suction pressure declined in the first min due to the depletion of refrigerant from the evaporator, and increased slowly due to the augmented refrigerant supply from the condenser before reaching its steady-state value. After the system was turned off, the suction and discharge pressures came to equilibrium quickly because of refrigerant migration from the condenser to the evaporator. It can be observed that the pressure transients with the 1st, 2nd and 4th variants were very close to those with the standard momentum equation, whereas the 3rd (dp/dt approach) and 5th (zero pressure drop) variants both over-predicted the pressures. When neglecting pressure drops across the heat exchangers, the mass flow rate of the circulating refrigerant increased, resulting in an enlarged pressure difference across the LEV to balance the refrigerant flow delivered by the compressor. Hence, both suction and discharge pressures rose and an over-prediction in pressures can be anticipated. However, the cause of over-prediction in pressures with the 3rd variant was non-obvious and needed to be carefully scrutinized. In this variant, the time derivative of the pressure was assumed to be uniform along the direction of refrigerant flow. This assumption is valid only when the pressure difference across the heat exchangers is small. Otherwise, it can be very easily violated under large disturbances, leading to errors in the mass calculation.

Fig. 4 showed the variations in the computed refrigerant mass inventory of the system during the entire simulation cycle. It was evident that refrigerant mass was well conserved with all the variants except the dp/dt approach. In order to eliminate the influence of numerical integration errors on the mass calculation, pressures and densities along with specific enthalpies were all selected as the dynamic states [12] in this work. Therefore, mass drift in the dp/dt approach was an inherent problem due to its underlying assumption. The refrigerant mass in the heat exchanger at time t can be computed as

$$M_{cal} = M_0 + \int_0^t \sum_{i=1}^n V_i \left(\frac{\partial \bar{\rho}}{\partial p} \frac{dp_{ref}}{dt} + \frac{\partial \bar{\rho}}{\partial \bar{h}_p} \frac{d\bar{h}_p}{dt} \right)_i dt \quad (18)$$

Table 1 Comparison of CPU time

Model Type	Standard	Steady-state	Friction only	dp/dt	Linear pressure	Zero pressure drop
CPU Time (s)	2855	592	111	214	175	165

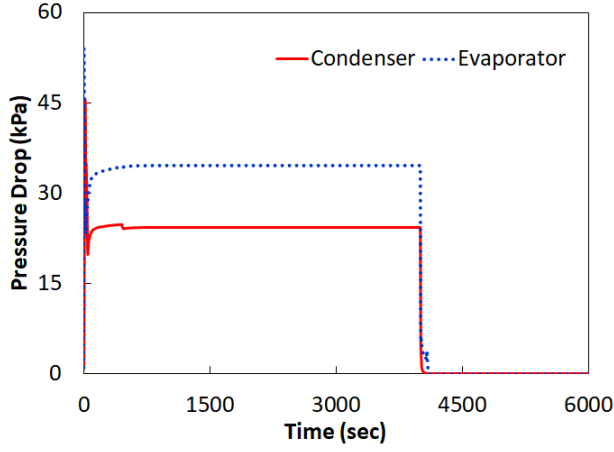


Fig. 5 Heat exchanger pressure drop with dp/dt approach.

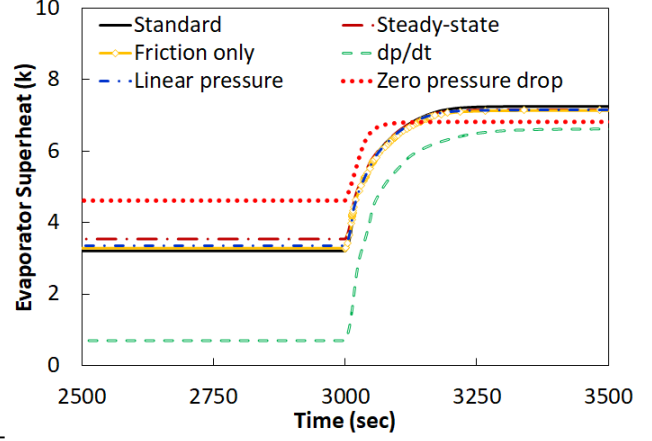


Fig. 6 Comparison of evaporator superheats.

with the initial mass M_0 . Assuming the inlet pressure of the heat exchanger is the reference pressure p_{ref} , the true refrigerant mass is

$$M_{true} = M_0 + \int_0^t \sum_{i=1}^n V_i \left[\frac{\partial \bar{\rho}}{\partial p} \frac{d(p_{ref} + \sum_{j=1}^{i-1} \Delta p_j)}{dt} + \frac{\partial \bar{\rho}}{\partial \bar{h}_p} \frac{d\bar{h}_p}{dt} \right] dt \quad (19)$$

where the pressure of the i^{th} control volume is $p_i = p_{ref} + \sum_{j=1}^{i-1} \Delta p_j$. Therefore, the amount of spurious mass drift is

$$\Delta M = M_{true} - M_{cal} = \int_0^t \sum_{i=1}^n V_i \left[\frac{\partial \bar{\rho}}{\partial p} \frac{d(\sum_{j=1}^{i-1} \Delta p_j)}{dt} \right] dt \quad (20)$$

According to Eq. (20), there should be no mass drift when the sum of pressure drops does not change over time. However, as shown in Fig. 5, refrigerant pressure drops spiked up from zero to 45 kPa and 55 kPa for the condenser and evaporator at the beginning of start-up, respectively, and then stabilized at 25 kPa and 32 kPa when the system reached the steady-state operation. After the system was powered off, refrigerant pressures equalized rapidly and pressure drops became zero. Comparing Fig. 5 and Fig. 4, it was clear that the variations in refrigerant mass synchronized with those in pressure drops across the heat exchangers. Therefore, the underlying assumption of the dp/dt approach was invalid when modeling the transients resulting from large disturbances.

The comparison of the CPU computation time with all different variants was shown in Table 1. The models with the simplified variants were significantly faster than the standard model. The increase in speed was achieved by neglecting the phenomena on a time scale much smaller than the one for the thermal phenomena of interest and the reduction in the number of dynamic states. Among these simplified variants, the one with the steady-state momentum balance was the slowest, whereas the one with only frictional pressure drop was the fastest.

Meanwhile, the impact of these different variants on the dynamic system response subject to a step change in the opening of the LEV was examined. Starting from steady-state operation, the LEV opening was reduced to 18% from 20% at 3000 sec. As shown in Fig. 6, when the LEV opening decreased, the resulting evaporator superheat increased due to the reduced refrigerant flow through the valve. Evaporator superheat from the

Table 2 Comparison of step response

Model Type	Standard	Steady-state	Friction only	dp/dt	Linear pressure	Zero pressure drop
Gain	202.10	181.05	192.95	296.05	190.05	110.15
Time Constant (s)	54.13	53.54	53.79	53.36	53.76	30.98

models with the 1st, 2nd and 4th variants corresponded well with those from the standard model, whereas the results from the models with the 3rd and 5th variants exhibited remarkable discrepancies. Table 2 listed the gain and time constant of the step response obtained from these different models, indicating that the variants with frictional pressure drop only and with linear pressure distribution produced the closest results to the standard model. However, the variant with zero pressure drop resulted in smaller gains and much faster responses, indicating that in some cases special care needed to be taken because the zero pressure drop assumption might lead to substantial errors in model-based control design.

4. CONCLUSIONS

Five simplified variants of the momentum equation that are often applied in the dynamic models of vapor compression systems were discussed in this article, and a complete cycle model of an air-source heat pump with these different approximations was developed in Modelica. In comparing the characteristics of these variants against the standard momentum equation, it is clear that the neglecting the phenomena on small time scales can greatly improve numerical efficiency while still preserving the physical integrity of cycle models. Among all these simplified momentum equations, the variants with frictional pressure drop only and with linear pressure distribution outperform the others, in the aspects of both prediction accuracy and simulation speed. Meanwhile, the dp/dt approach exhibits spurious mass drift under large disturbances due to its underlying assumption. When the mass drift issue becomes a concern, special treatments are needed to ensure that refrigerant mass is conserved, for instance, adding a refrigerant filling component with neutral enthalpy to the system model. Moreover, a comparison of the dynamic evaporator superheat response subject to a step change in the valve opening indicates that the zero pressure drop assumption could lead to faster dynamics and smaller changes in the steady-state outputs.

REFERENCES

- [1] C. Schulze. *A contribution to numerically efficient modelling of thermodynamic systems*. PhD thesis, Technische Universitt Braunschweig, Institut fr Thermodynamik, 2013.
- [2] J.J. Brasz and K. Koenig. Numerical methods for the transient behavior of two-phase flow heat transfer in evaporators and condensers. *Numerical Properties and Methodologies in Heat Transfer*, pages 461–476, 1983.
- [3] C.C. Richter. *Proposal of new object-oriented equation-based model libraries for thermodynamic systems*. PhD thesis, Technische Universitt Braunschweig, Institut fr Thermodynamik, 2008.
- [4] J.M. Jensen. *Dynamic modeling of thermo-fluid systems with focus on evaporators for refrigeration*. PhD thesis, Technical University of Denmark, Department of Mechanical Engineering, 2003.
- [5] S.A. Bendapudi, J.E. Braun, and E.A. Groll. Dynamic model of a centrifugal chiller system - model development, numerical study, and validation. *ASHRAE Trans*, Part I:132–148, 2005.
- [6] W. Zhang and C. Zhang. On three forms of momentum equation in transient modeling of residential refrigeration systems. *Int. J. Refrigeration*, 32:938–944, 2009.
- [7] S. Levy. *Two-phase flow in complex systems*. New York: John Wiley & Sons, 1999.
- [8] S.V. Patankar. *Numerical heat transfer and fluid flow*. New York: Hemisphere Publishing Corporation, Taylor and Francis Group, 1980.
- [9] H. Qiao, V. Aute, and R. Radermacher. Transient modeling of a flash tank vapor injection heat pump system - part i: Model development. *Int. J. Refrigeration*, 49:169–182, 2015.
- [10] H. Qiao, C. Laughman, D. Burns, and S. Bortoff. Dynamic characteristics of an r410-a multi-split variable refrigerant flow air-conditioning system. In *12th IEA Heat Pump Conference*. Rotterdam, Netherlands, 2017.
- [11] S. Levy. Forced convection subcooled boiling prediction of vapor volumetric fraction. *Int. J. Heat Mass Transfer*, 10:951–965, 1967.
- [12] C. Laughman and H. Qiao. On the influence of state selection on mass conservation in dynamic vapor compression cycle models. *Math Comput Model Dyn Syst*, 23:262–283, 2017.